

O. Holm-Hansen · C.D. Hewes · V.E. Villafañe
E.W. Helbling · N. Silva · T. Amos

Distribution of phytoplankton and nutrients in relation to different water masses in the area around Elephant Island, Antarctica

Received: 28 October 1996 / Accepted: 20 January 1997

Abstract During January–March 1996 the U.S. Antarctic Marine Living Resources program carried out an extensive multidisciplinary study in a 40,000 km² sampling grid around Elephant Island, Antarctica. The physical, chemical, optical, and biological characteristics of the upper water column (0–750 m) were determined at 91 hydrographic stations. Analysis of the temperature and salinity data showed that six different hydrographic zones could be differentiated. The biological (phytoplankton distribution and abundance) and chemical (inorganic nutrient concentrations) data also showed characteristic differences within each of these six zones. In spite of high concentrations of inorganic N, P, and Si in all six zones, all stations in the northwest portion of the sampling grid (Drake Passage waters) showed very low chlorophyll-*a* concentrations in surface waters and a sub-surface maximum at increased depth. As stations in this zone have a relatively stable upper mixed layer of 40 m, excess macro-nutrients, and adequate solar radiation for maximal photosynthetic rates, this suggests that rates of primary production in this zone are limited by a micro-nutrient such as Fe. Phytoplankton abundance was much greater in the Bransfield Strait, in waters influenced by Bellingshausen Sea Water, and in the frontal zones where these water masses mix with Drake Passage waters. Relatively low and deeply distributed phytoplankton abundance was found at all stations in the southeastern portion of

our sampling grid, where the upper water column was very weakly stratified and showed the characteristics of Weddell Sea water. The areas of enhanced phytoplankton biomass in the AMLR sampling grid roughly correspond to the areas where krill are generally also found in greater abundance. The overall biological productivity of the Elephant Island region would thus appear to be dependent upon the circulation patterns of the major water masses that intrude into this area.

Introduction

The physical oceanographic characteristics of the area around Elephant Island, Antarctica are complex due to mixing of different water masses, effects of islands, and the variable bottom topography that ranges from large continental shelf areas to deep pelagic waters. As this is one of the major areas for the commercial harvesting of krill (Nicol and de la Mare 1993; SC-CCAMLR 1994), it is important to better understand the food reservoirs that support these large krill populations. The geographical distribution and abundance of phytoplankton in this area, as well as rates of primary production, show great variability from month to month and also interannually (Helbling et al. 1995). Since the area around Elephant Island includes waters coming from the Bellingshausen Sea, Bransfield Strait, Weddell Sea, and Drake Passage, considerable variation can be expected in the physical, chemical, and optical characteristics in the water column, depending upon the source of the water mass.

On the basis of analysis of physical oceanographic data over a 7-year period, Amos (1997) has recently described six different geographical water zones in the area around Elephant Island, each of which can be characterized by the shape of the temperature/salinity diagram for the upper water column. There are, of course, some seasonal and interannual variations in the geographical boundaries defining these six water zones. In early 1996, the U.S. Antarctic Marine Living Re-

O. Holm-Hansen (✉) · C.D. Hewes · V.E. Villafañe · E.W. Helbling
Polar Research Program, Scripps Institution of Oceanography,
University of California, San Diego,
La Jolla, CA 92093-0202, USA
Fax: 619-534-7313

N. Silva
Escuela de Ciencias del Mar, Universidad Católica
de Valparaíso, Valparaíso, Chile

T. Amos
University of Texas at Austin, Marine Science Institute,
Port Aransas, TX 78373, USA

sources (AMLR) program conducted extensive physical and biological studies in a large sampling grid centered around Elephant Island. Data from the AMLR program have been used in this paper to determine if the distribution and abundance of phytoplankton can be related to the different physical and chemical conditions found within each of these six water zones and thus to the geographical origin of the water within each of the zones.

Materials and methods

The sampling grid around Elephant Island consisted of 91 hydrographic stations (Fig. 1), which included stations in relatively shallow continental shelf regions and also in deep pelagic areas. The 91 stations were occupied sequentially during the time period January 23–February 4 1996.

At each station an instrumented rosette was deployed to 750 m (or to within a few meters of the bottom when the depth was less than 750 m), with data being recorded on both the down and up casts. In addition to eleven 10-liter Niskin water-sampling bottles equipped with Teflon-covered springs, the following sensors were mounted on the rosette: (1) a Sea-Bird model SBE-9 PLUS CTD, (2) an ORI 12-kHz pinger, (3) a 25-cm beam transmissometer (Sea Tech), (4) an irradiance sensor (BSI, model # QCP-200L) for photosynthetically available radiation (PAR), and

(5) a pulsed fluorometer (Sea Tech) for estimation of chlorophyll-*a*. All data from the CTD unit were recorded by computer.

Water samples were obtained on the up cast at standard depths of 5, 10, 15, 20, 30, 40, 50, 75, 100, and 200 m. Water was drained directly from the Niskin bottles into acid-cleaned plastic bottles (polycarbonate or polyethylene) for the following analyses:

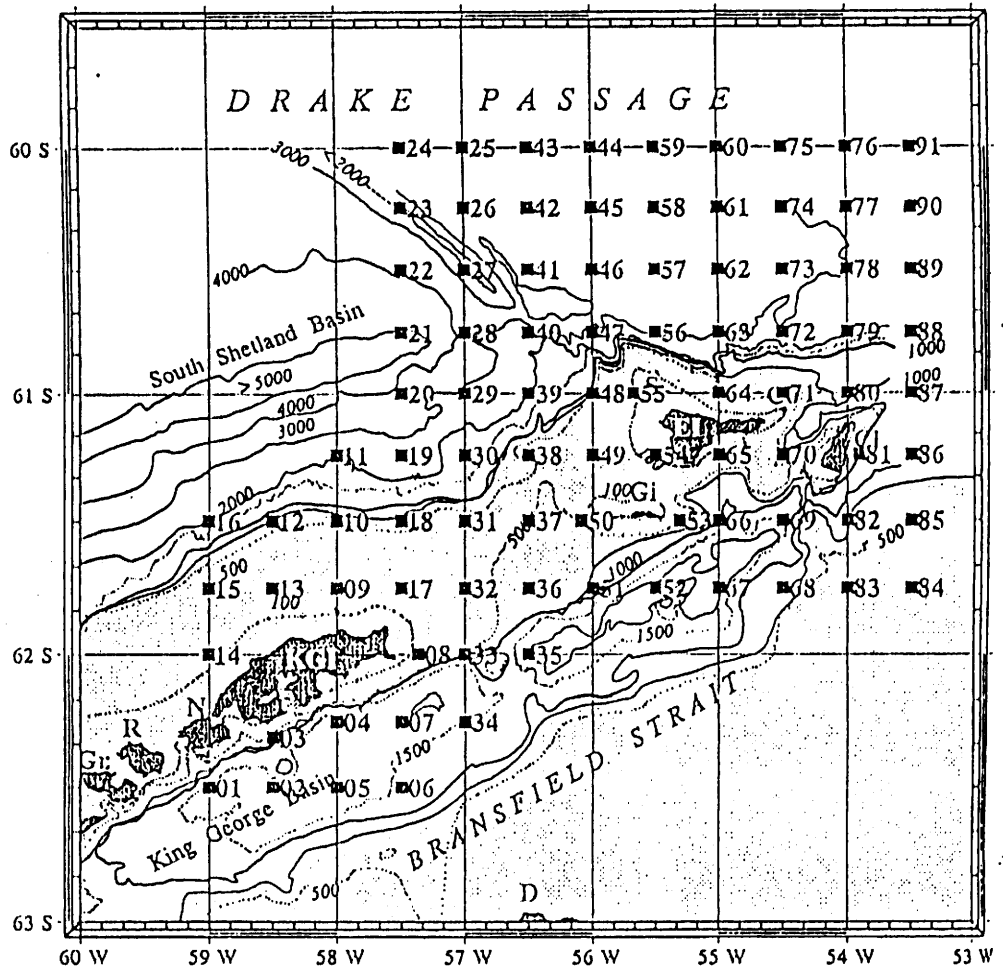
(1) For measurement of chlorophyll-*a* (chl-*a*), samples (100 ml) were filtered at a pressure differential < 150 mm Hg through a 25-mm glass fiber filter (Whatman GF/F), which was then placed in 10 ml absolute methanol in a glass-stoppered centrifuge tube (Holm-Hansen and Riemann 1978). After extraction in the dark for at least 4 h, chl-*a* concentrations were calculated by measurement of chl-*a* fluorescence (Holm-Hansen et al. 1965) in a Turner Designs fluorometer (model 10-005R), which had been calibrated against purified chl-*a* (Sigma C-6144) and the instrument response checked daily with a coproporphyrin standard (Sigma C-4529).

(2) Samples for nutrient analyses (75 ml) were collected in acid-cleaned (1N HCl) polyethylene bottles and maintained at -20°C until analysis. An autoanalyzer was used for determination of nitrate + nitrite, phosphate, and silicic acid (Atlas et al. 1971). Throughout this paper we will refer to the concentration of nitrate + nitrite as nitrate concentration.

Results

Analyses of the temperature (*T*) and salinity (*S*) profiles at the 91 stations in the AMLR sampling grid showed

Fig. 1 Map of the AMLR sampling grid, showing the location of each of the 91 numbered stations. Depth isopleths (m) are also shown. The areas where the depth is less than 750 m are shaded. Islands within the sampling grid include Greenwich Island (*Gr*), Robert Island (*R*), Nelson Island (*N*), King George Island (*KGI*), Gibbs Island (*Gi*), Elephant Island (*EI*), and Clarence Island (*CI*)



that six geographical zones could be identified, each of which could be characterized by the shape of the T/S diagrams. These six characteristic T/S diagrams are shown in Fig. 2, together with maps showing the geographical area for each of the six water zones. The chief characteristics of the upper water column (0-750 m) within each of these water zones are:

Zone 1 Drake Passage stations, characterized by warm, low-salinity surface water, a strong sub-surface temperature minimum (generally < 0°C), and a T/S maximum near 500 m. Major water masses include Antarctic Surface Water (AASW) and Circumpolar Deep Water (CDW).

Zone 2 A transition water zone with surface waters having higher salinity than in zone 1 and a broader temperature minimum at approximately 80-m depth.

Major water masses include AASW and CDW, which show some mixing with shelf waters.

Zone 3 This zone also includes AASW and CDW, but the relatively few stations in this zone can be differentiated from zones 1 and 2 by a broad temperature minimum generally below 100-m depth and no CDW temperature maximum around 500-m depth.

Zone 4 Eastern Bransfield Strait stations, with surface waters slightly cooler and more saline than in zones 1-3. Temperature generally decreases continuously with depth, with no temperature-minimum layer close to 100 m; bottom waters close to -1°C. Water masses include AASW, CDW, and Bransfield Strait deep water.

Zone 5 Waters in this zone are typical of the physical characteristics of Weddell Sea water. Surface waters are

Fig. 2a-f T/S diagrams characterizing each of the water zones identified within the AMLR sampling grid. The heavy line in each sub-figure is the mean of all the individual T/S diagrams, which are shown as lighter lines (the mean has been omitted for zone #6 as there are so few stations in that area). The numbers on the diagrams refer to the depth (m) at various points along the T/S diagrams. The maps to the right of each T/S diagram show the location of the stations that are found within each of the six characteristic water zones

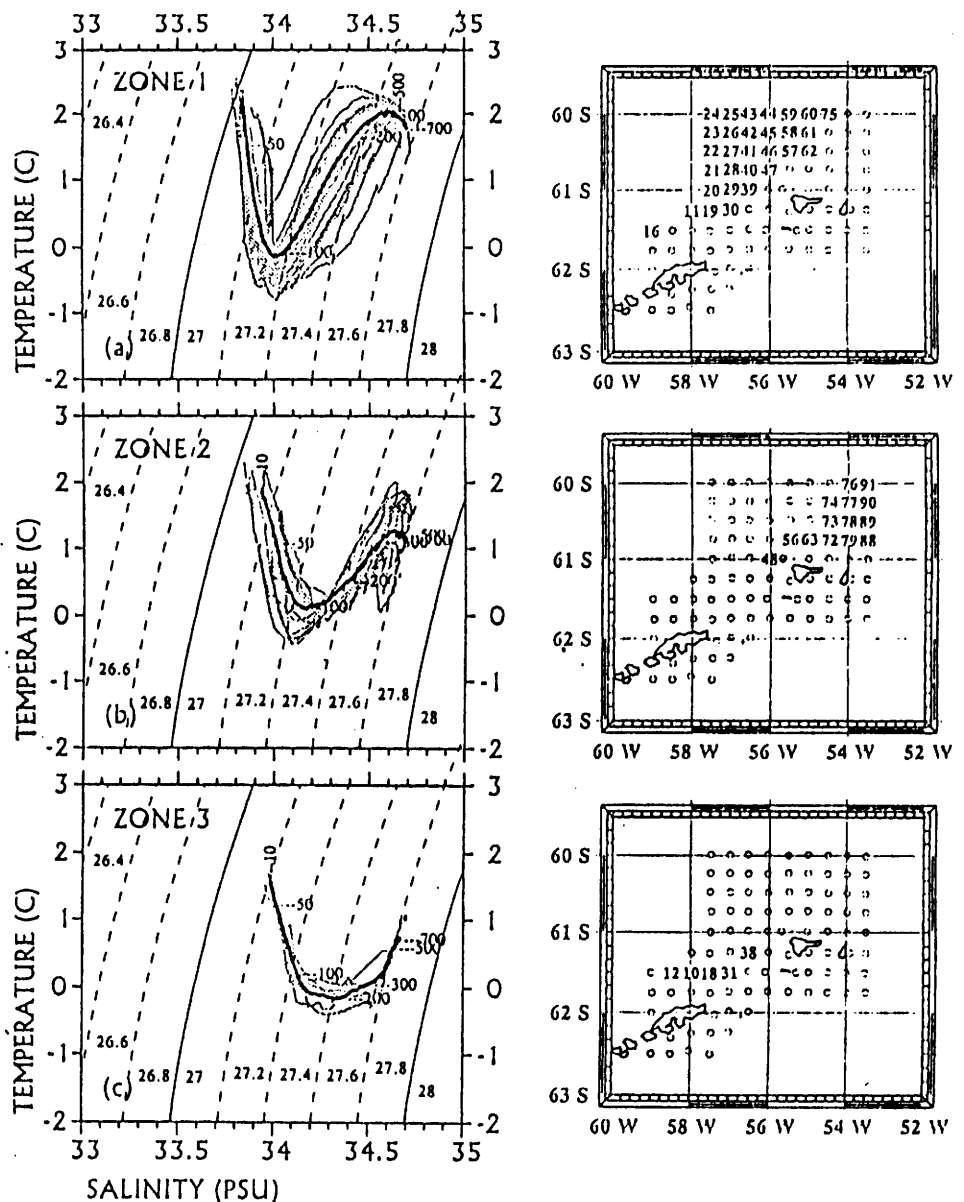


Fig. 2a-c

colder and more saline than in zones 1-4. The water column is weakly stratified and shows little vertical structure.

Zone 6 The relatively few stations within this zone represent shallow shelf stations close to Elephant Island or King George Island, and are grouped together as they do not fit in any of the other five water zones. The water columns show little vertical structure.

The mean profiles of water density (σ_t) for the upper 200 m of the water column for all stations within each of the six water zones are shown in Fig. 3. A relatively stable upper mixed layer (UML) of approximately 40-m depth characterizes stations in zone 1. Stations in zone 3 show weaker stratification, but with an UML of approximately 35-m depth. In the remain-

ing zones (zones 2, 4, 5, and 6) there was no well defined UML as the water density increases continuously with depth. The least stable water columns are found in zones 5 and 6.

Examination of the concentrations of chl-a in the upper 200 m of the water column in each of the above water zones (Fig. 4) shows that zone 1 had very low chl-a concentrations as compared to the other five water zones and also that there was a sub-surface maximum at approximately 20-m depth. Chl-a concentrations were highest in zone 2, with the maximal values (mean of $1.9 \mu\text{g l}^{-1}$) at or close to the surface, with concentrations decreasing quite rapidly with increasing depth. The profiles of chl-a concentrations in zones 3-5 were fairly similar to that in zone 2, but the maximal values ($1.0-1.3 \mu\text{g l}^{-1}$) were lower than in zone 2. Stations

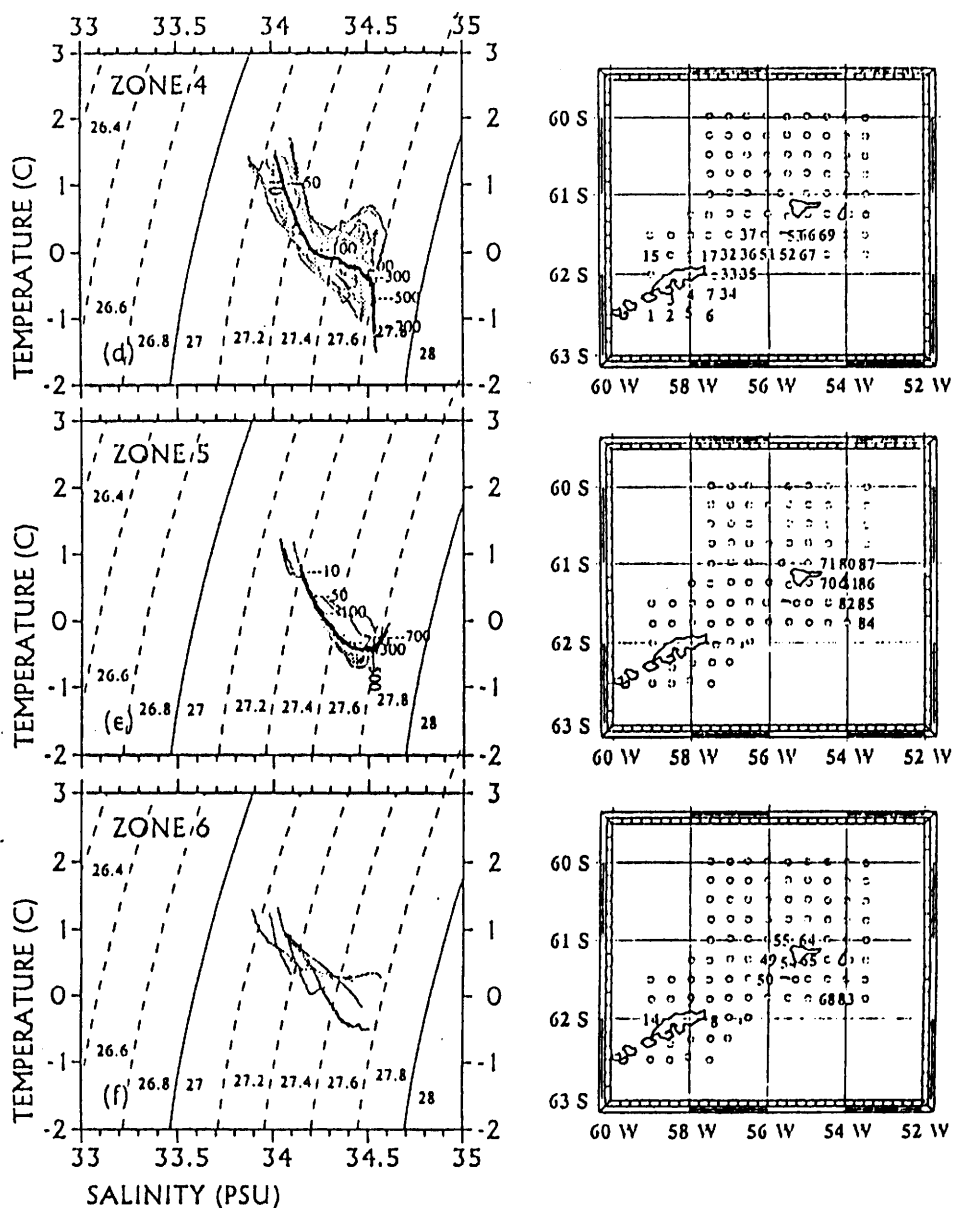


Fig. 2d-f

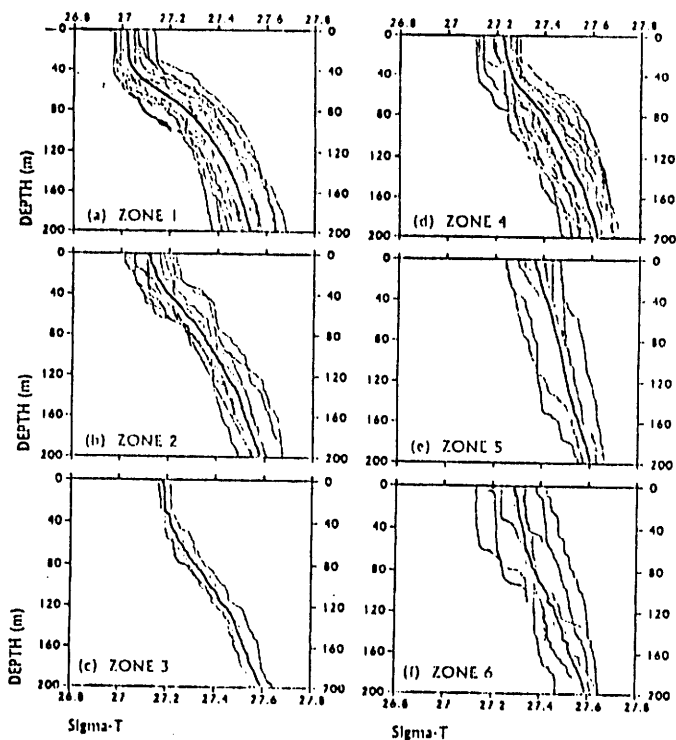


Fig. 3a-f Mean profiles (*heavy line*) of water density ($\sigma\text{-t}$) in the upper water column at all stations included within each of the six identified water zones. The *lighter lines* show the individual profiles of $\sigma\text{-t}$ for each station

within water zone 6 show maximal but low concentrations of chl-a ($0.8 \mu\text{g l}^{-1}$) close to the surface, with concentrations decreasing relatively slowly with depth. The depths of the euphotic zone (surface to depth where solar irradiance is 1% of incident PAR) in the various water zones were generally between 65 and 75 m (zone 1), 40 and 45 m (zone 2), 40 and 50 m (zone 4), 50 and 60 m (zone 5), and 60 and 65 m (zone 6). There were insufficient data to report the depth of the euphotic zone for zone 3 as the five stations in this zone were occupied during night-time.

Previous studies (Villafañe et al. 1993) have shown that transmissometer data are a very good indicator of phytoplankton biomass expressed in cellular organic carbon. Data in Fig. 5 show the mean beam transmission values in percent as determined with the transmissometer mounted on the profiling CTD array. The highest percent beam transmission values, both in surface waters and below 100 m were in zone 1, in agreement with the low chl-a values in this zone. The lowest beam transmission values in the upper 40 m of the water column were in zone 2, followed by zones 3 and 4. In zones 5 and 6 the profiles of the beam transmission values were quite high and increased slowly from the surface to 200 m, thus resembling the chl-a profiles seen in Fig. 4.

The sub-surface chl-a maximum at approximately 20-m depth for all the stations in zone 1 was surprising,

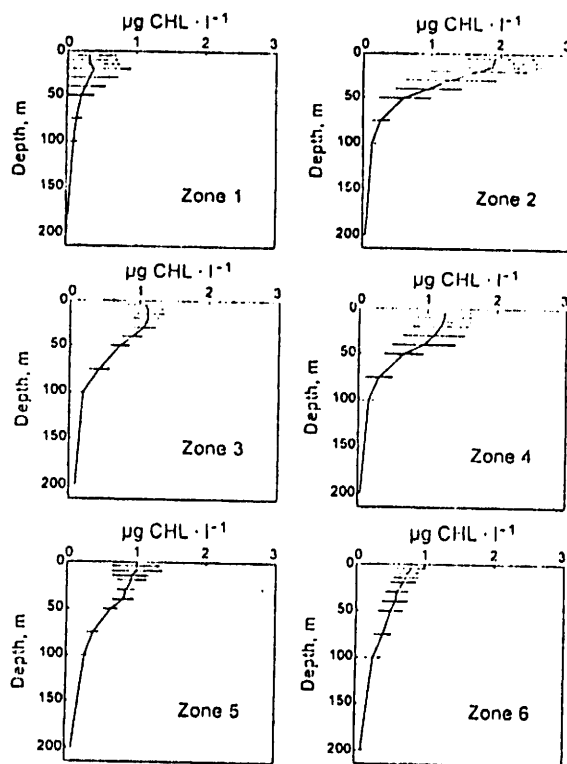


Fig. 4 Mean concentrations of chl-a in the upper water column at all stations included within each of the six identified water zones. The *horizontal lines* show the standard deviation from the mean

as these pelagic waters to the north and northwest of Elephant Island usually have a chl-a maximum at close to 80-m depth (Holm-Hansen et al. 1994). The individual chl-a profiles for each of these stations were thus examined and it was apparent that the stations in zone 1 could be broken down into two groups, with each group showing a mean chl-a profile that was characteristic of all stations in that subgroup but that was different from the mean chl-a profile in the other sub-group (Fig. 6). Stations in sub-group 1A had very low chl-a concentrations ($<0.1 \mu\text{g l}^{-1}$) in surface waters, and a sub-surface maximum (approximately $0.13 \mu\text{g l}^{-1}$) at approximately 80-m depth. Stations in sub-group 1B had much higher chl-a concentrations in the upper 20 m of the water column (approximately $0.8 \mu\text{g l}^{-1}$), below which the concentrations decreased rapidly.

The stations in the sub-groups 1A and 1B could also be differentiated on physical and optical characteristics of the upper water column (Fig. 7). The T/S diagrams and profiles of water density for stations in the 1A sub-group are very similar to those for zone 1 stations (Figs. 2, 3) whereas the T/S diagrams and profiles of water density for stations in the 1B sub-group are intermediate between those for zones 1 and 2. The mean profile of beam transmission values for stations in the 1A sub-group (Fig. 7) shows considerably higher values (and thus lower biomass) than the mean profile for all stations in zone 1 (Fig. 2); the mean profile for stations

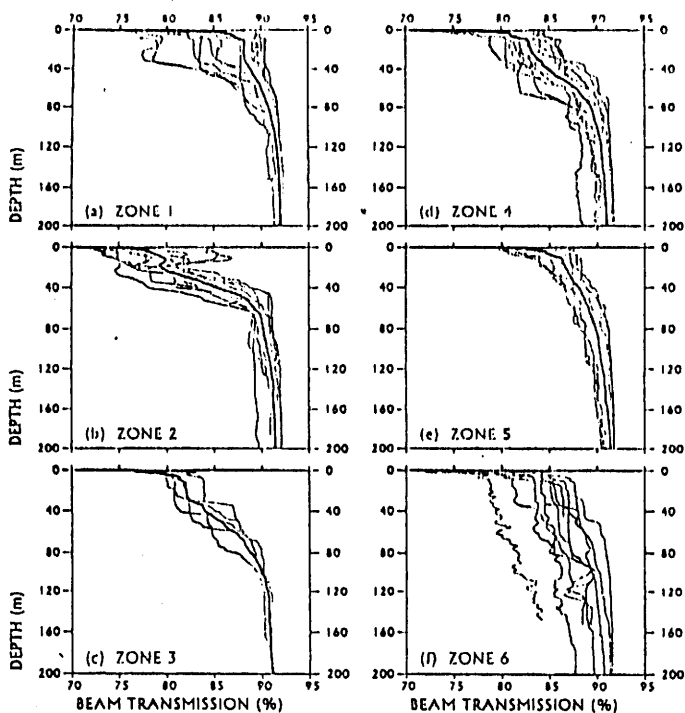


Fig. 5a-f Profiles of beam transmission (in percent) in the upper water column at all stations included within each of the six identified water zones. The heavy line in each sub-figure is the mean of all the individual profiles, which are shown as lighter lines (the mean has been omitted for zone #6 as there are relatively few stations in that area and there is considerable variability)

in the 1B sub-group is intermediate between the mean profiles in zones 1 and 2.

The above data suggest that the distribution and abundance of phytoplankton in the Elephant Island area may be influenced by the physical and chemical characteristics of the various water masses that flow through the AMLR study area. Nutrient analyses showed that the concentrations of inorganic nitrogen ($> 22 \mu\text{M}$), phosphorus ($> 1.6 \mu\text{M}$), and silicic acid ($> 36 \mu\text{M}$) are all high in all six water zones and are well above the concentrations that are thought to limit phytoplankton growth rates (Table 1). Chl-a values, however, differed markedly between some of the water zones, as the 5-m and integrated values in zone 1A were only 5% and 20%, respectively, of those in zone 2.

As the major water masses influencing the AMLR area have slightly different nutrient concentrations in addition to characteristic temperature and salinity profiles, the nutrient data were analyzed to see if the six described water zones could also be differentiated by their nutrient concentrations or nutrient ratios (Fig. 8). When mean phosphate concentrations are plotted against nitrate concentrations (Fig. 8A) or silicic acid concentrations (Fig. 8B) for the various water zones, it is seen that the stations in sub-groups 1A, 1B, and in zone 2 tend to group together, as do stations in zones 3 and 4 and stations in zones 5 and 6. Values for stations in sub-groups 1A and 1B are separated from each other, particularly in respect to silicic acid concentrations. All three nutrients (N, P, Si) show maximum concentra-

Fig. 6 Mean concentrations of chl-a in the upper water column at all stations included within zones 1A and 1B. Note the change of scale on the abscissa. The horizontal lines show the standard deviation from the mean. The maps above show the location of the stations that are found within zones 1A and 1B

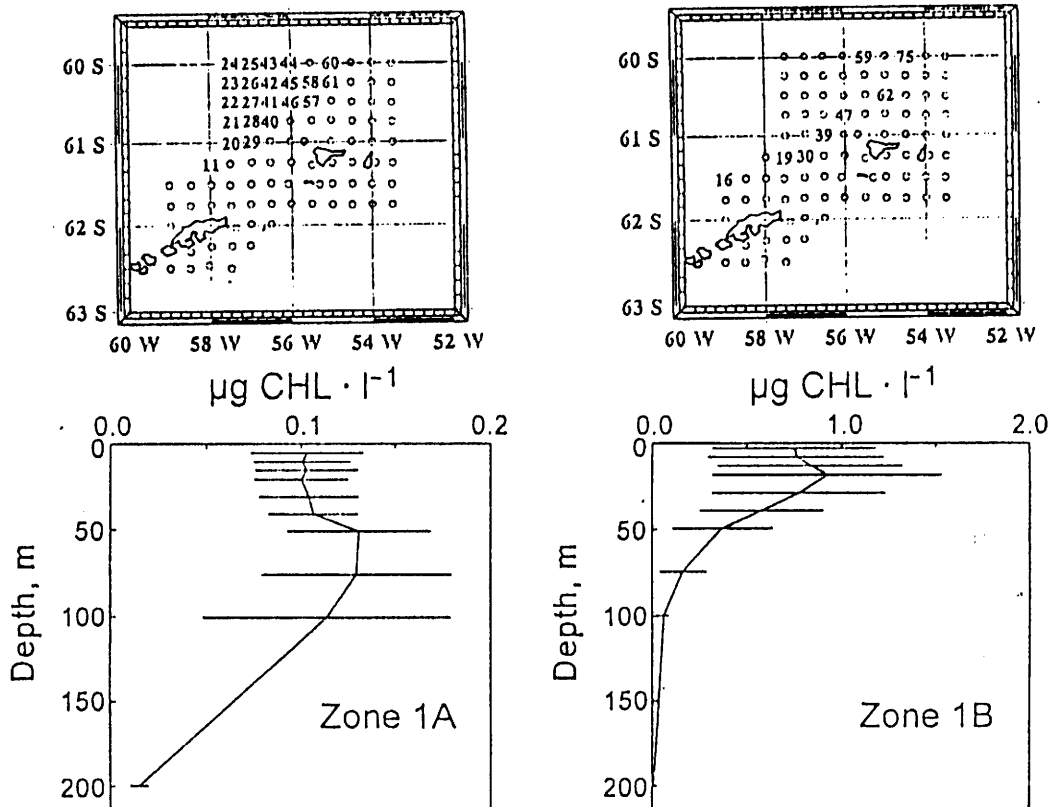
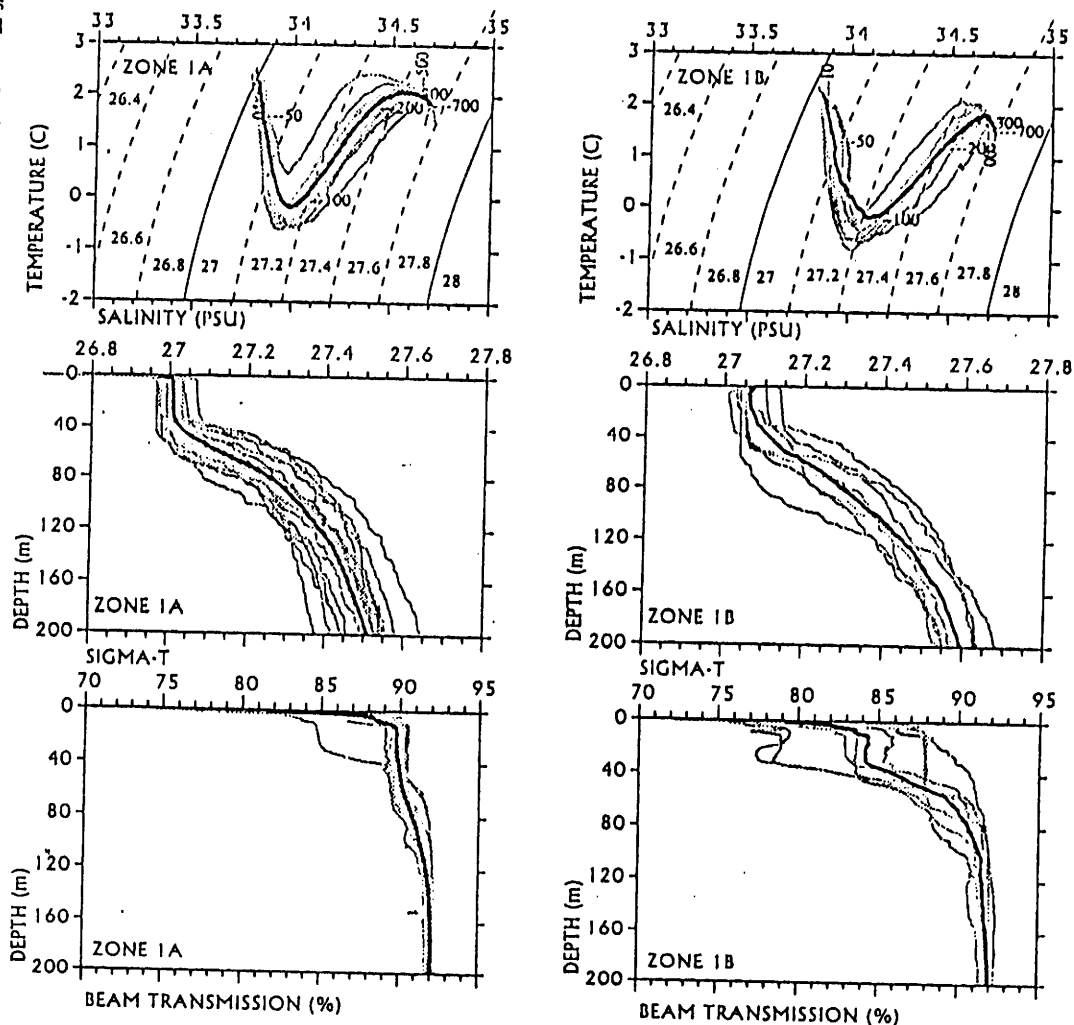


Fig. 7 Physical (T/S diagrams and water density) and optical (percent beam transmission) characteristics of the upper water column in zones 1A and 1B. The heavy line in each sub-figure is the mean of all the individual profiles, which are shown as lighter lines



tions in zones 5 and 6. When phosphate concentrations are plotted against chl-a concentrations at 5-m depth (Fig. 8C), it is seen that sub-group 1A and 1B are distinct from the other five water zones. There is a fairly good linear relationship between integrated chl-a values and 5-m chl-a concentrations in the various water zones (Fig. 8D), with stations in subgroup 1A spatially distinct from the other six zones.

Discussion

Our data show that the demarcation for the six characteristic geographic zones described by Amos (1997) for the AMLR sampling grid on the basis of physical characteristics of the water column are apparently also relevant in regard both to phytoplankton distribution and abundance and to nutrient status of the upper water column in these six zones. Zone 1 is clearly very

Table 1 Chlorophyll-*a* and inorganic nutrient concentrations in the six different water zones found within the AMLR study area around Elephant Island, Antarctica

Water zone	n	5 m mg CHL · l ⁻³	0-200 m mg CHL · m ⁻²	Nutrient (μM) at 5-m depth		
				PO ₄	NO ₃	Si(OH) ₄
1	31	0.31 ± 0.39	25.4 ± 17.9	1.72 ± 0.09	23.4 ± 1.62	42.7 ± 11.0
1A	21	0.10 ± 0.03	16.5 ± 5.0	1.74 ± 0.09	23.8 ± 1.63	36.6 ± 6.2
1B	10	0.75 ± 0.43	44.1 ± 20.7	1.68 ± 0.09	22.7 ± 1.28	55.4 ± 7.5
2	12	1.90 ± 0.59	82.1 ± 29.4	1.76 ± 0.09	24.0 ± 1.52	65.9 ± 6.04
3	5	1.01 ± 0.26	68.5 ± 9.3	1.87 ± 0.03	25.3 ± 0.55	76.6 ± 0.49
4	20	1.27 ± 0.40	73.1 ± 18.2	1.83 ± 0.06	24.9 ± 0.69	77.5 ± 2.01
5	9	0.98 ± 0.36	73.0 ± 11.2	1.98 ± 0.10	28.0 ± 1.54	80.9 ± 1.29
6	13	0.80 ± 0.21	66.5 ± 13.2	2.00 ± 0.07	27.3 ± 1.15	77.9 ± 2.06

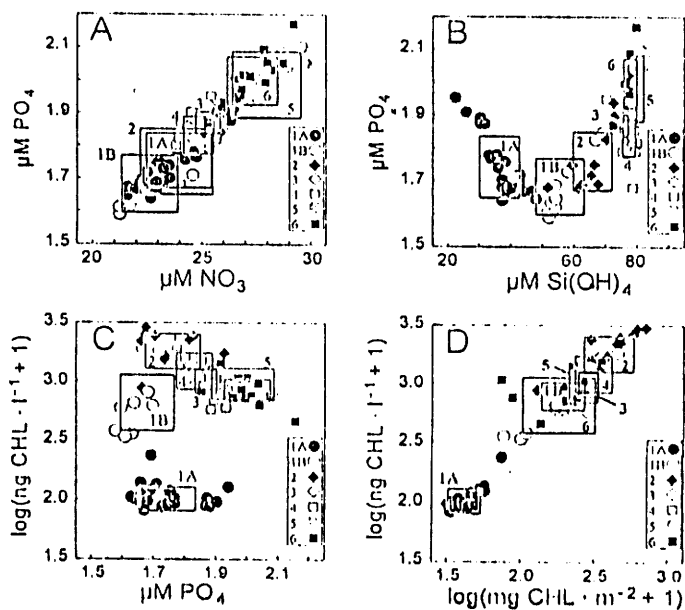


Fig. 8A–D Nutrient and chl-a relationships in the six water zones within the AMLR sampling area. Nutrient concentrations are all at 5-m depth. The rectangular boxes indicate the standard deviations about the mean values for all stations within each zone. A nitrate concentrations regressed against phosphate concentrations; B silicic acid concentrations regressed against phosphate concentrations; C phosphate concentrations regressed against chl-a concentrations at 5-m depth; D integrated chl-a concentrations (0–200 m) regressed against chl-a concentrations at 5-m depth

different from the other five zones as stations in that zone have very low phytoplankton biomass, a sub-surface maximum in chl-a concentrations, and very low silicic acid concentrations. Stations in zones 2–4 all have fairly high chl-a concentrations, which are maximal at or close to the surface, but the nutrient data (Fig. 8) show that stations in zone 2 are most similar to zone 1 stations, whereas concentrations of N, P, and Si are fairly uniform in zones 3 and 4 but higher than in zone 2. The highest nutrient concentrations are found in zone 5, which reflects the influence of the nutrient-rich outflow from the Weddell Sea. Chl-a concentrations within this zone, however, are fairly low and are more deeply distributed than in stations in zones 2–4. Stations in zone 6, which are relatively shallow and show weaker density stratification than the other five zones, have the lowest phytoplankton biomass, which decreases slowly with depth.

Although the physical characteristics of the water column suggested that all stations within zone 1 should be grouped together, examination of the chl-a data from these stations clearly showed that there were two well-delineated groups within zone 1 that could be described on the basis of chl-a concentrations, as well as the profile of chl-a with depth. When the physical data of these two sub-groups were analysed, it was apparent that the biological and physical characteristics of stations in zone 1B reflected the mixing of waters of zone 2 with Drake Passage waters, which characterize stations

in zone 1A. This effect of mixing is apparent in the physical (σ_t/S diagrams and profiles of water density), optical (beam transmission values), nutrient (particularly Si), and biological (chl-a distribution and abundance) features of the stations in zone 1B.

Phytoplankton blooms ($> 1\text{--}2 \mu\text{g chl-a l}^{-1}$) in Antarctic waters are generally found only when there is a well-developed UML that is sufficiently shallow, so that the mean irradiance to which phytoplankton are exposed in the UML permits a rapid increase of biomass. Both field data (Mitchell and Holm-Hansen 1991) and mathematical models (Sakshaug et al. 1991) suggest that a UML of 40 m in which there is no nutrient limitation of phytoplankton growth should be able to develop a phytoplankton crop of close to $5 \mu\text{g chl-a l}^{-1}$. The profiles of water density in the six zones of the AMLR grid show that a well-defined and relatively shallow and stable UML is found in zone 1, and that stations in zone 3 have a less stable UML of approximately the same depth. Profiles of σ_t in the other four zones do not show any well-defined UML, but instead show that water density increases continuously with depth. One would thus expect stations in zone 1 to have higher phytoplankton crops than in the other water zones. On the contrary, however, stations in zone 1 have very low concentrations of chl-a. There is obviously some factor(s) that is limiting phytoplankton biomass in zone 1. As the physical, optical, and macro-nutrient (N, P, Si) conditions in zone 1 would seem to be optimum for phytoplankton growth, the most likely growth-controlling factor is an essential micro-element such as Fe. This suggestion is well supported by measurement of dissolved Fe in shallow and deep waters of Antarctica (de Baar et al. 1990), as well as by Fe-addition growth experiments of natural Antarctic phytoplankton assemblages in the AMLR study area (Helbling et al. 1991). In contrast to waters in zone 1, available data in the literature would indicate that there should be relatively high Fe concentrations in the waters found within the other five zones. (Martin et al. 1990). The low phytoplankton biomass in zone 1 and the correspondingly low rates of primary production in this zone (Helbling et al. 1995) thus seem to result from concentrations of available iron that are controlling phytoplankton growth.

With the mixing of shelf waters (presumably with sufficient dissolved iron to permit maximal phytoplankton growth rates) with zone 1 waters (with low iron concentrations), one would expect that the physical, chemical, and optical conditions in the upper portion of the water column within the mixing zone would result in elevated phytoplankton biomass and increased rates of primary production. Stations within this mixing region (zone 1B) are seen to lie on the periphery of zone 1 and do indeed show much higher phytoplankton concentrations than throughout zone 1A (Figs. 4, 6). Previous studies (Helbling et al. 1993) have also described dramatically elevated phytoplankton biomass in the region encompassing some of our

zone 1B stations, but in those studies the reason for the increased phytoplankton biomass was discussed only in relation to changes in profiles of water column stability.

Data from previous AMLR cruises have shown that areas of high krill abundance (e.g. see Fig. 4.3 in Loeb et al. 1995) generally also have relatively high phytoplankton biomass (Villafañe et al. 1995). Conversely, our stations in zone 1A have very low concentrations of chl-a and generally also show very low concentrations of krill as shown by acoustic data (Hewitt et al. 1996). This positive correlation between phytoplankton and krill biomass is not surprising as it has been shown previously that dense swarms of krill in the area north of Elephant Island are actively feeding (Antezana and Ray 1984) and hence must depend upon adequate rates of primary production. The distribution and abundance of phytoplankton (and hence concomitant rates of primary production) in the Elephant Island area, however, vary considerably in the six water zones, which can be distinguished from each other on both physical and chemical characteristics. The geographical extent of these different zones (particularly zones 1-3), which can be expected to be dependent upon variations in the flow patterns of the various water masses found in the AMLR study area, will thus strongly influence the distribution and abundance of phytoplankton and, in turn, the distribution and abundance of grazing zooplankton such as krill. Thus both seasonal and long-term climate changes (e.g., global warming) that affect physical dynamic processes can be expected to influence stock sizes of higher trophic levels as a result of changes in phytoplankton productivity.

Acknowledgements This work was supported by NOAA Contract No. 50ABNF600013. We thank all officers and crew of the R/V *Yuzhmorgeologiya* for their excellent support during all field operations, and also all other AMLR personnel who assisted us on board ship.

References

- Amos AF (1997) Hydrography of the Elephant Island, Antarctica area: water masses and geostrophy. In: Jacobs S (ed) Antarctic Research Series: Coastal shelf dynamics. American Geophysical Union, Washington, DC
- Antezana T, Ray K (1984) Active feeding of *Euphausia superba* in a swarm north of Elephant Island. *J Crust Biol* 4:142-155
- Atlas EL, Gordon LI, Hager SW, Park PK (1971) A practical manual for the use of the Technicon Autoanalyzer in seawater nutrient analyses: revised. Technical Report 71-22. Oregon State University, Department of Oceanography
- Baar HJW de, Buma AGJ, Nolting RF, Cadee GC, Jacques G, Treguer PJ (1990) On iron limitation of the Southern Ocean: experimental observation in the Weddell and Scotia Seas. *Mar Ecol Prog Ser* 65:105-122
- Helbling EW, Villafañe VE, Holm-Hansen O (1991) Effect of Fe on productivity and size distribution of Antarctic phytoplankton. *Limnol Oceanogr* 36:1879-1885
- Helbling EW, Amos AF, Silva N, Villafañe VE, Holm-Hansen O (1993) Phytoplankton distribution and abundance as related to a frontal system north of Elephant Island, Antarctica. *Antarct Sci* 5:25-36
- Helbling EW, Villafañe VE, Holm-Hansen O (1995) Variability of phytoplankton distribution and primary production around Elephant Island, Antarctica, during 1990-1993. *Polar Biol* 15:233-246
- Hewitt R, Mitchell E, Demere D, Chavez GV, Holt R (1996) Bioacoustic survey: In: Martin J (ed) AMLR 1995/96 field season report LJ-96-15. Southwest Fisheries Science Center, La Jolla
- Holm-Hansen O, Riemann B (1978) Chlorophyll-a determination: improvements in methodology. *Oikos* 30:438-447
- Holm-Hansen O, Lorenzen CJ, Holmes RW, Strickland JDH (1965) Fluorometric determination of chlorophyll. *J Cons Perm Int Explor Mer* 30:3-15
- Holm-Hansen O, Amos AF, Silva M, Villafañe VE, Helbling EW (1994) In situ evidence for a nutrient limitation of phytoplankton growth in pelagic Antarctic waters. *Antarct Sci* 6:315-324
- Loeb V, Nebenzahl D, Outram D, Force M, Phleger R, Rosenberg J, Setran A, Shigenaka G, Zapata C (1995) Direct krill and zooplankton sampling. In: Rosenberg J (ed) AMLR 1994/95 Field Season Report LJ-95-13. Southwest Fisheries Science Center, La Jolla
- Martin JH, Gordon RM, Fitzwater SE (1990) Iron in Antarctic waters. *Nature* 345:156-158
- Mitchell BG, Holm-Hansen O (1991) Observations and modeling of the Antarctic phytoplankton crop in relation to mixing depth. *Deep Sea Res* 38:981-1007
- Nicol S, Mare W de la (1993) Ecosystem management and the Antarctic krill. *Am Sci* 81:36-47
- Sakshaug E, Slagstad D, Holm-Hansen O (1991) Factors controlling the development of phytoplankton blooms in the Antarctic Ocean - a mathematical model. *Mar Chem* 35:259-271
- SC-CCAMLR (1994) Report of the Thirteenth Meeting of the Scientific Committee, Commission for the Conservation of Antarctic Marine Living Resources. Hobart
- Villafañe VE, Helbling EW, Holm-Hansen O (1993) Phytoplankton around Elephant Island, Antarctica: distribution, biomass and composition. *Polar Biol* 13:183-191
- Villafañe VE, Helbling EW, Holm-Hansen O, Montes M (1995) AMLR program: horizontal and vertical distribution of phytoplankton biomass in the vicinity of Elephant Island during January-March 1995. *Antarct J US* 30:232-234